UNIVERSITY OF CALIFORNIA
ENGINEERING AND SCIENCES EXTENSION SERIES

Balakrishnan · Space Communications
Beckenbach · Modern Mathematics for the Engineer, First Series
Beckenbach · Modern Mathematics for the Engineer, Second Series
Brown and Weiser · Ground Support Systems for Missiles and Space Vehicles
Dorn · Mechanical Behavior of Materials at Elevated Temperatures
Garvin · Natural Language and the Computer
Huberty and Flock · Natural Resources
Langmuir and Hershberger · Foundations of Future Electronics
LeGalley and McKee · Space Exploration
Leondes · Computer Control Systems Technology
Leondes · Guidance and Control of Aerospace Vehicles
Parker · Materials for Missiles and Spacecraft
Puckett and Ramo · Guided Missile Engineering
Ridenour · Modern Physics for the Engineer, First Series
Ridenour and Nierenberg · Modern Physics for the Engineer, Second Series
Robertson · Modern Chemistry for the Engineer and Scientist
Sines and Waisman · Metal Fatigue
Zarem and Erway · Introduction to the Utilization of Solar Energy

SPACE EXPLORATION

Robert M. L. Baker, Jr.
Herbert C. Corben
Paul Dergarabedian
Manfred Eimer
Louis B. C. Fong
A. Donald Goedeke
Maxwell W. Hunter, II
William W. Kellogg
Lewis Larmore
Donald P. LeGalley
Colin J. Maiden
John L. Mason
Robert E. Roberson
Morris Tepper
Robert M. Wood

Edited by

Donald P. LeGalley

TRW Space Technology Laboratories
Space Technology Center
Redondo Beach

John W. McKee

General Electric Company—TEMPO
Santa Barbara

1964

McGRAW-HILL BOOK COMPANY

New York, San Francisco, Toronto, London

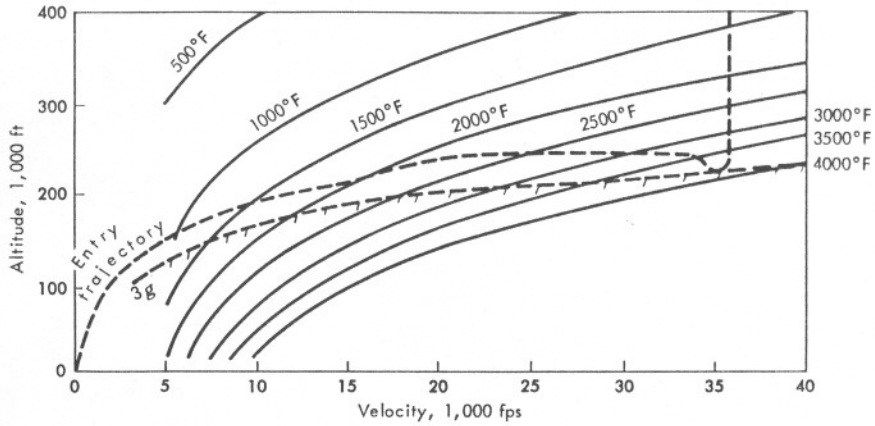

Fig. 10-8 Venus equilibrium temperatures for a 10-ft-radius stagnation point, emissivity = 0.8.

It should again be stressed that in this chapter all thermal results pertain only to the stagnation point of a 10-ft-radius nose. Although this appears somewhat restrictive, it is generally true that, if there is a thermal design problem at the nose, there is a thermal design problem elsewhere, and since an objective of this chapter is to discuss design trends, the selection of the stagnation point appears both reasonable and simple.

10-4 Mission Constraints and Requirements

The only reason for carefully considering thermostructural problems related to high-speed entry to the planets is because the entry speeds are high enough to lead to these problems (Ref. 17). Approach and entry speeds can be easily reduced to any value preferred by the use of propulsive braking. The system advantage rests in the potential weight savings afforded by the elimination of propulsion unit or propellant weight. Thus, a lighter vehicle is expected if a little thermal protection is added, saving considerable propulsion weight. The potential of this can be clearly seen in Eq. (10-4), where it is anticipated that a given impulsive velocity can be eliminated (the approach velocity), corresponding to a lot of W_P, at the expense of adding only a little W_S.

$$V_I = gI_{sp} \ln \frac{W_G}{W_E} \qquad \text{where } \frac{W_G}{W_E} = (W_P + W_S + W_{PL})/(W_E + W_{PL}) \tag{10-4}$$

This may be true even for low-thrust interplanetary vehicles, for which the thrust is presumed less than the weight (on all three planets). For such systems, the atmosphere can be used to brake the vehicle to orbital

energy, which is probably worth looking at even at specific impulses of, say, 5,000 sec. Equation (10-4) contains the essence of all major compromises in rocketry: V_E and W_{PL} (mission objective), I_{sp} (performance efficiency), and W_S (structural and engine efficiency or weight penalty). The use of atmospheric braking reduces the V_I required, and if the increase in W_S required to do this is small enough, we are clearly ahead and take the benefit in either larger payload or less propellant, or smaller gross, or a combination. Chapter 12 (Hunter) points out how atmospheric braking would significantly enhance the potential of nuclear rockets (Ref. 17).

A representative mission is shown in Fig. 10-9, which uses a fairly optimistic timetable. Such a timetable would clearly require a nuclear-propulsion unit and one of high thrust for the mission dates involved. The impulsive-velocity requirements for this mission and a comparable Venus mission are given in Table 10-5, which has been computed on the assumption of planetary entry by atmospheric braking. The small velocity shown opposite "Retro" is only for the purpose of decreasing the entry speed to an acceptable value for accuracy.

The kinematics of the orbital transfer and the selection of the stay time on the planet dictate a connection between the total round-trip transfer time and the impulsive velocity required to accomplish the mission. This is shown in Fig. 10-10, where the minimum total velocity refers to the selection of the most favorable date for that minimum

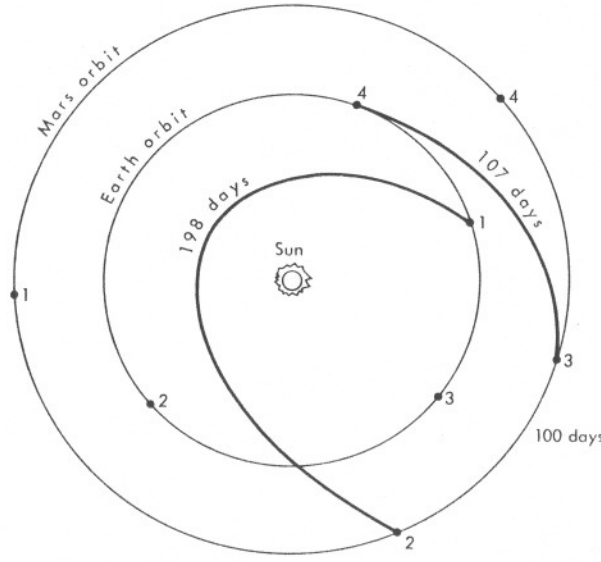

Fig. 10-9 Typical Earth-Mars round-trip mission. (1) Nov. 6, 1971; (2) May 23, 1972; (3) Aug. 30, 1972; (4) Dec. 15, 1972.

Table 10-5 Impulsive-velocity Requirements, Round-trip Missions (In fps)

Mission phase	Mars*	Venus†
Launch velocity	25,000	25,000
Exit losses	13,800	13,800
Velocity added at orbit	39,000	15,400
Retro at destination	7,000	500
Planetary landing	700	500
Return launch	33,000	38,500
Exit losses	4,000	8,500
Retro at Earth	3,500	5,000
Earth landing	400	400
Midcourse guidance	2,000	2,000
Space radiation, reactor radiation, planetary radiation propellant, losses	6,400	7,200
Total impulsive velocity, fps	134,800	116,800

* 100-day stay time.
† 30-day stay time.

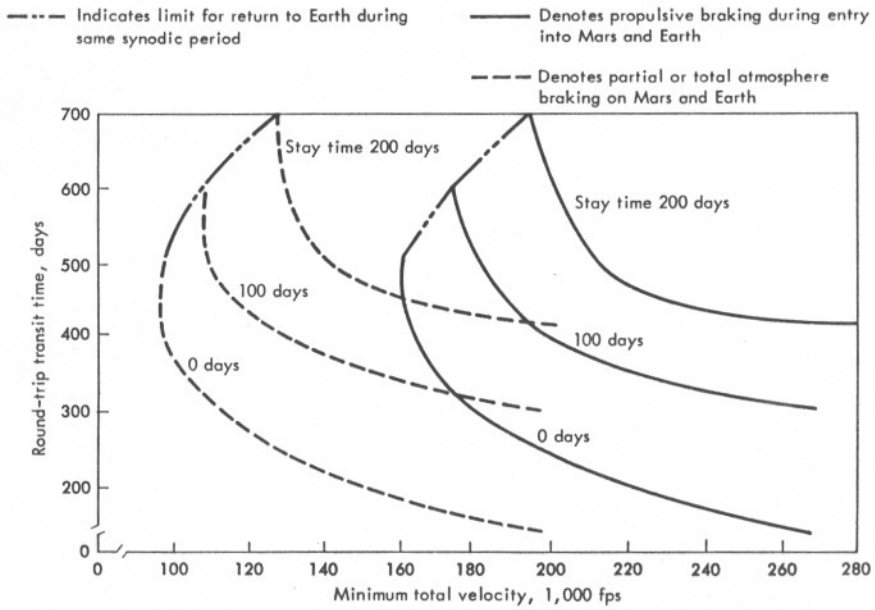

Fig. 10-10 Minimum total velocity for a given round-trip time to Mars. Earth and Mars velocity losses and midcourse guidance corrections included.

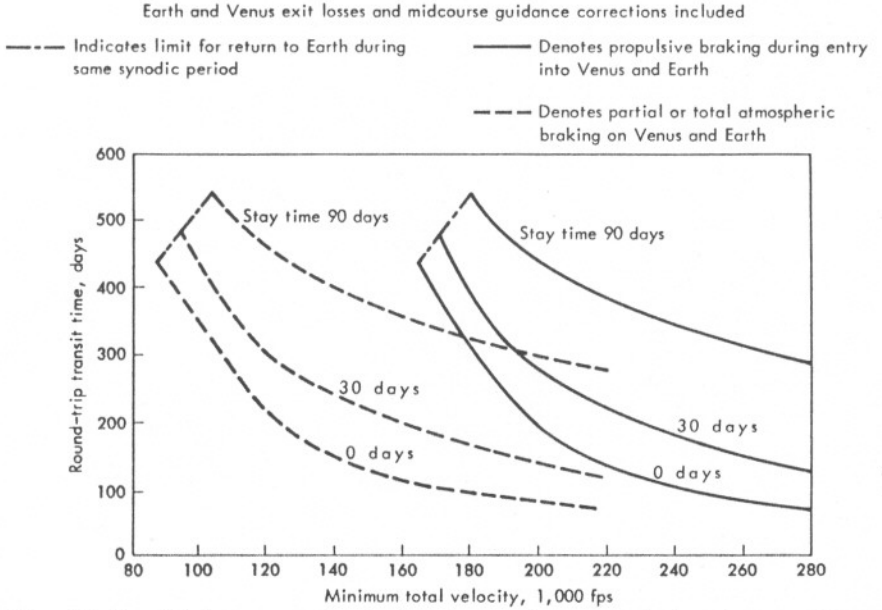

Fig. 10-11 Minimum total velocity for a given round-trip time to Venus. Earth and Venus velocity losses and midcourse guidance corrections included.

energy within the restriction of stay time and transit time. Figure 10-11 gives comparable results for Venus. These results are not intended to represent a meticulous study, for they are based on two-dimensional transfer orbits. They are, however, valid for exemplifying the order of magnitude of total velocity required, with and without atmospheric braking, shown by the dashed lines. The impulsive velocity saved by the use of atmospheric braking is of the order of 60,000 to 70,000 fps for both Mars and Venus.

Just as the kinematics of the orbital transfer implies the relation shown in Figs. 10-10 and 10-11, the same considerations require the approach speeds to the planets shown in Figs. 10-12 and 10-13. It should be noted that, for a round-trip time of about 400 days, a 100-day stay time on Mars corresponds to an approach and entry velocity of 35,000 fps and a 30-day stay time on Venus corresponds to an approach velocity of 40,000 fps. Both values are considerably in excess of escape velocity for the respective planets.

If we are to focus our attention on a *manned* entry vehicle, then the acceleration tolerance of the man becomes critical in the design and selection of the entry system. If we keep in mind that a simple interpretation of the physiological data would lead to the desirability of not exceeding a fixed number of g, it is possible to compare the entry corridor for ballistic-entry, drag-modulation, and lifting-entry vehicles. This is

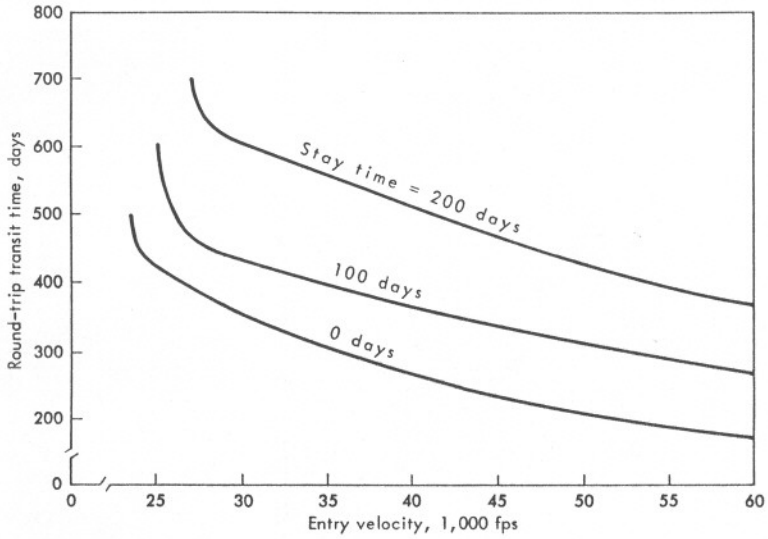

Fig. 10-12 Martian entry velocities for minimum total velocities for a given round-trip time; entry altitude = 800,000 ft.

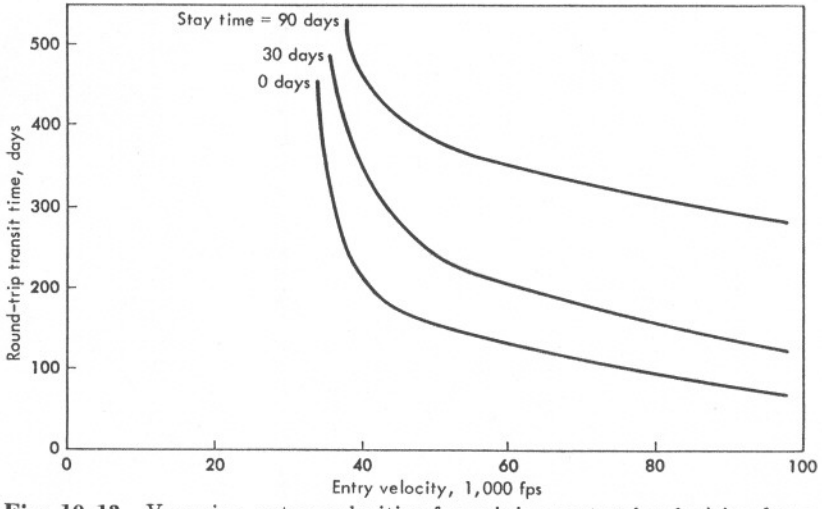

Fig. 10-13 Venusian entry velocities for minimum total velocities for a given round-trip time; entry altitude = 400,000 ft.

done for Earth in Fig. 10-14. Figure 10-14*a* gives the relationship between the allowable range of entry angles and the entry velocity for a ballistic entry. Entry angles larger than those in the white sliver lead to excessive g, and smaller entry angles lead to either a skip or an escape. If drag modulation is considered in Fig. 10-14*a*, wherein a large

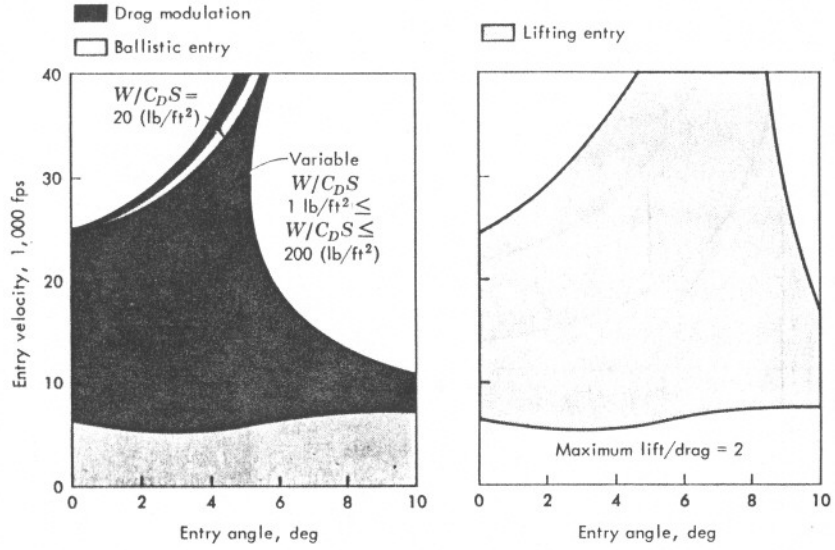

Fig. 10-14 Entry corridors afforded by several modes of entry; maximum deceleration of 6 g is not exceeded.

area of drag opens at high altitude and becomes smaller as the speed and altitude go down during entry, it appears that the entry corridor is opened up drastically. Since the addition of another variable, namely, drag, is of some help, we would also expect that the addition of lift as a variable would be of help. This fact is shown in Fig. 10-14*b*, where now the entry corridor for not exceeding 6 g is even wider. Another way of illustrating the favorable effect of lift is shown in Fig. 10-15, which shows that the maximum g occurring during entry for a given set of conditions decreases with increasing lift-to-drag ratio.[1] It is apparent that a little lift goes a long way in reducing the g; however, this is an oversimplification of the interaction, for it does not treat the influence of the other variables of vehicle-entry design.

Figure 10-16 presents the variation of dynamic pressure (a measure of the loads on the vehicle) and heat-rate potential, $\rho u^3/2$ (a measure of the heat severity) for a ballistic-entry vehicle.

Figure 10-17 gives the same information for a lifting-entry vehicle selected to be comparable in overall size. It should be noted that the maximum loads have been reduced by a factor of 15 and the thermal problem reduced by a factor of 25. In summary, a manned entry to the planets at high speed demands a lifting vehicle. A lifting vehicle is necessary because it reduces the g, because it widens the entrance corridor

[1] At $L/D = 0$, the 35,000 fps case has lower g than the 25,600 fps case because the entry angle for minimum g is much smaller at the higher speed.

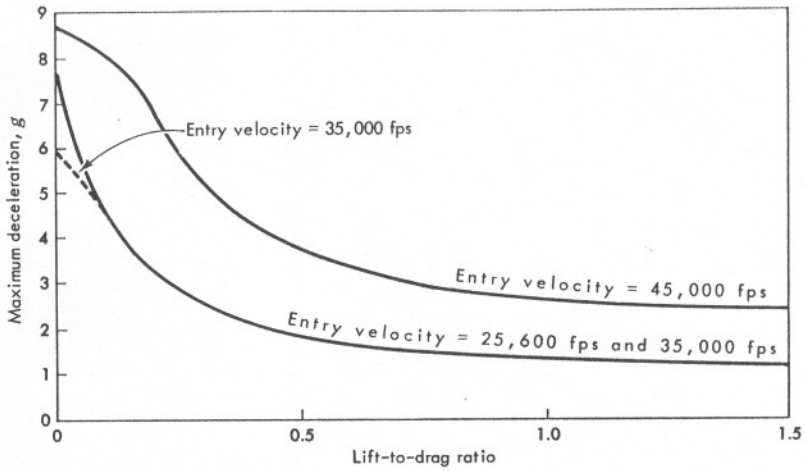

Fig. 10-15 Influence of lift-drag ratio on maximum deceleration; entry altitude = 400,000 ft.

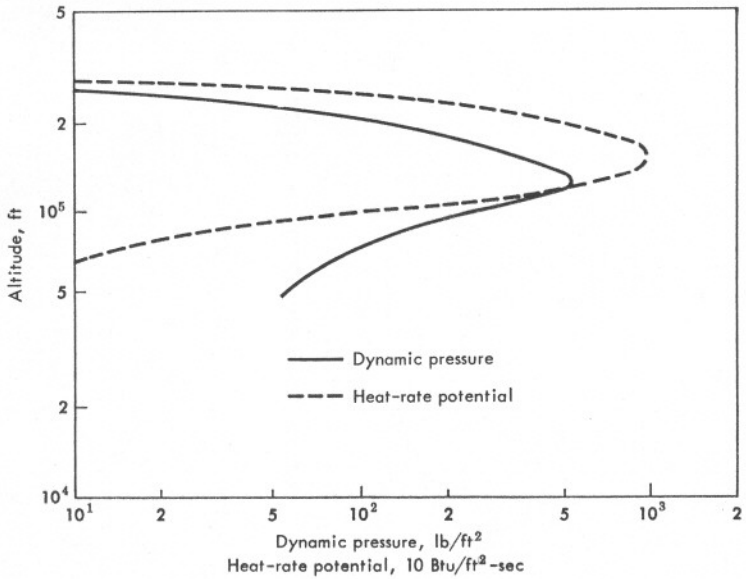

Fig. 10-16 Pressure and heating for ballistic entry; W/C_DS = 50 psf, V_E = 25,000 fps, $\gamma_E = -3°$.

and reduces the guidance-accuracy requirements, because it reduces the loads and the attendant structural weight, and because it reduces the heating and the attendant thermal-protection weight. For all these reasons among manned entry vehicles we shall consider only those with lift.

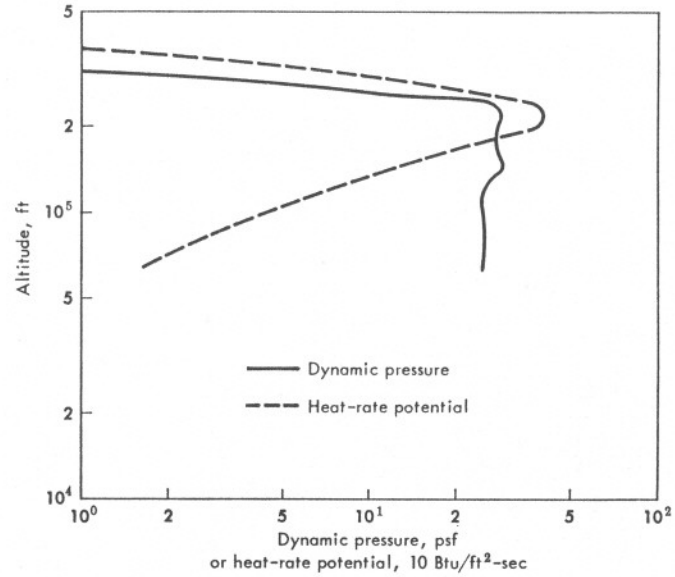

Fig. 10-17 Pressure and heating for lifting entry; W/C_LS = 31.8 psf, V_E = 25,800 fps, $\gamma_E = -1°$.

10-5 Vehicle Shapes and Entry Dynamics

The next question is what kind of lifting-vehicle configurations are worthy of consideration. Figure 10-18 shows the three representative shapes: the upper left shape corresponds to a high-drag blunted cone (Ref. 17); the middle shape has a thick wing, with surfaces added for lateral stability, and has a higher lift-to-drag ratio; the last shape has a much thinner, lower-drag lifting delta wing. Each of these configurations will have a lift and drag coefficient associated with them as a function of angle of attack, where the relationship between the lift and drag is determined by a curve such as that shown in Fig. 10-19, corresponding to the upper left configuration of Fig. 10-18. A particular point on a lift-drag polar is determined by the angle of attack of the vehicle, which therefore controls the relationship between lift and drag within this limitation. At this stage of design considerations, it is worthwhile not only to consider how a particular vehicle shape could be made to perform during entry but also to imagine that that shape is variable. Within this broader framework, therefore, the emphasis in this section will be placed on how the independent kinematic and shape parameters influence the dependent variables of interest indicated in Table 10-6.

The variables mentioned in Table 10-6 are directly or indirectly of design interest because of the intimate relationship to either the mission requirements or the ultimate weight of the vehicle. The differential